Hindawi Publishing Corporation
International Journal of Photoenergy
Volume 2012, Article ID 716087, 10 pages
doi:10.1155/2012/716087

Research Article

Neodymium-Doped TiO_2 with Anatase and Brookite Two Phases: Mechanism for Photocatalytic Activity Enhancement under Visible Light and the Role of Electron

Douga Nassoko,[1] Yan-Fang Li,[1] Jia-Lin Li,[1] Xi Li,[2,3] and Ying Yu[1]

[1] *Institute of Nanoscience and Nanotechnology, Central China Normal University, Wuhan 430079, China*
[2] *Jiangsu Huannengtong Environment Protection Co. Ltd, Zhenjiang 212006, China*
[3] *Zhenjiang King Lithium Cell Co. Ltd, Zhenjiang 212006, China*

Correspondence should be addressed to Ying Yu, yuying@phy.ccnu.edu.cn

Received 14 August 2011; Accepted 30 September 2011

Academic Editor: Jiaguo Yu

Titanium dioxide (TiO_2) doped with neodymium (Nd), one rare earth element, has been synthesized by a sol-gel method for the photocatalytic degradation of rhodamine-B under visible light. The prepared samples are characterized by X-ray diffractometer, Raman spectroscopy, UV-Vis diffuse reflectance spectroscopy, X-ray photoelectron spectroscopy, and Brunauer-Emmett-Teller measurement. The results indicate that the prepared samples have anatase and brookite phases. Additionally, Nd as Nd^{3+} may enter into the lattice of TiO_2 and the presence of Nd^{3+} substantially enhances the photocatalytic activity of TiO_2 under visible light. In order to further explore the mechanism of photocatalytic degradation of organic pollutant, photoluminescence spectrometer and scavenger addition method have been employed. It is found that hydroxide radicals produced by Nd-doped TiO_2 under visible light are one of reactive species for Rh-B degradation and photogenerated electrons are mainly responsible for the formation of the reactive species.

1. Introduction

Dye wastewater discharged into nature mainly by dyestuff, textile industry, and some artificial way causes severe ecological problems. These compounds are highly colored and can heavily contaminate water source. Chemical oxidation method for dye wastewater treatment is too costly and physical adsorption method often results in secondary pollution [1]. Many attempts have been carried out to develop efficient biological methods to decolorize these effluents but they have not been very successful. Semiconductor TiO_2 as a photocatalyst has been deeply investigated and can successfully degrade various organic pollutants [2–6]. However, the overall efficiency achieved so far with TiO_2-based systems is not sufficiently high to enable practical applications. This low efficiency is mainly due to the fast recombination of charge carriers produced by irradiated TiO_2 and thus the low quantum yield in the generation of reactive species for organic degradation [7, 8]. Moreover, due to its large bandgap (~3.2 eV), all photo-driven applications of TiO_2 require ultraviolet light excitation. As a consequence, TiO_2 shows photocatalytic activities under only a small fraction (<5%) of solar irradiation [9], limiting its practical applications. Therefore, the modification of TiO_2 to enhance light absorption and photocatalytic activities under visible light has been the subject of recent research [10].

Many factors that influence the photodegradation efficiency of organic pollutants over TiO_2 have been reported during the past 30 years. The main focus is the physical properties of TiO_2, including crystal phases, crystal facets, crystallinity, particle size, surface area, porosity, and morphology. It is not easy to make a reliable correlation between the structure and photoactivity of TiO_2 because the solid physical properties often affect one another. In general, anatase is considered to be much more active than rutile, while a mixture of anatase and rutile, like Degussa

P25, is claimed to be more active than anatase. So far, TiO_2 with anatase and brookite phases as a photocatalyst has been rarely studied because brookite TiO_2 has no activity for organic pollutant degradation and it needs higher temperature to prepare. Moreover, there has been little report about brookite TiO_2 preparation at low temperature.

The investigations about introducing foreign species are in progress for improving the photocatalytic activity of TiO_2 and broadening its absorption to solar spectrum. Among them, titania doped with metals or metallic cations such as transition metallic cations, rare metal cations, and noble metal have been widely explored [11, 12]. On one hand, these doped metallic cations tend to serve as recombination centers. As a result, in most cases, photoexcited charges are recombined by the sites of doping metallic cations [13]. On the other hand, it has been reported that suitable amount of metallic cation doping can promote the separation of photogenerated electrons for the improvement of photocatalytic activity [14, 15]. It is obvious that there is conflict. So, although there are quite a few publications about metal-doped TiO_2, the mechanism for the improvement of photocatalytic activity has not been clear so far. It needs explore in detail.

In this paper, to explore the mechanism of photodegradation of organic pollutant by rare earth element-doped TiO_2, neodymium (Nd) ion was selected as a TiO_2 dopant due to its stability to form complexes with various Lewis bases in the interaction of these functional groups with f-orbitals of neodymium metal [16]. Thus, incorporation of Nd ion into a TiO_2 matrix could provide an effective method to concentrate the organic pollutant at semiconductor surface. Here, Nd-doped TiO_2 samples were prepared by sol-gel method together with pure TiO_2 for comparison. The characteristics and properties of these photocatalyst were studied. The photocatalytic activity was evaluated by measuring photodegradation efficiency of rhodamine-B (Rh-B) under visible light. The photocatalytic mechanism of Nd-doped TiO_2 was also investigated in detail by photoluminescence spectrometer (PL) [17] and scavenger addition method [18].

2. Experimental Section

2.1. Materials. The chemicals used in this experiment except P25 were all analytical reagent and purchased from Shanghai Guoyao Chemical Co. Pure TiO_2, P25, was commercial product from Germany. The used water throughout the whole research was double-distilled water.

2.2. Experimental Procedure. Neodymium-doped TiO_2 samples (Nd-doped TiO_2) were prepared by sol-gel method. First, 5 mL of $TiCl_4$ was dissolved and hydrolyzed with 200 mL distilled frozen water (0°C). Second, Nd_2O_3 with certain amount required for doping was suspended into a small amount of ethanol and then added to the above solution to produce transparent Nd^{3+} aqueous solution under vigorous stirring. Third, 10 M NaOH aqueous solution was added dropwisely into the transparent $TiCl_4$ aqueous solution with Nd^{3+} to obtain a grey precipitate with an ultimate suspension of pH = 10.

In order to remove residual Na^+ and Cl^- ions, the precipitate was adequately washed with deionized water till the pH value of filtrated water was below 7. Then, the amorphous Nd-doped TiO_2 was well dispersed into 400 mL of water, and chloride acid (20%) was added with corresponding amount. The above suspension was adjusted to pH 1.5, stirred for 4 hours at room temperature, and then had been aged at 70°C for 24 h in airproof condition. Finally, Nd^{3+}-modified TiO_2 sol was formed with uniform, stable, and semitransparent characteristics. The obtained sol can maintain homogenous distribution for a long time without sedimentation and delamination. Powder sample was prepared by aging, gelation, and vacuum-drying treatment of the above sol at 70°C for 8 hours. TiO_2 sample was also prepared by the same procedure without the addition of the neodymium oxide suspension. The pure TiO_2 and Nd-doped TiO_2 samples were annealed in air at 400°C for 3 hours and ground to fine particles for different analysis.

2.3. Characterization of Photocatalysts. The crystalline phases of the synthesized TiO_2 and Nd-doped TiO_2 catalyst were analyzed by a Y-2000 diffractometer (D/max 30 kV) using graphite monochromatic copper radiation (Cu Kα) (λ = 0.154178 nm) at a scan rate of $0.06^\circ\ 2\theta \cdot s^{-1}$ at 40 kV, 40 mA over the diffraction angle range of $10 \sim 60^\circ$. Raman spectroscopy measurements were performed by using a Jobin Yvon Lab RAM HR 800UV micro-Raman system under an Ar^+ (514.5 nm) laser excitation. UV-Vis diffuse reflectance spectra (DRS) were recorded with a PerkinElmer Lambda 35 Spectrophotometer. X-ray photoelectron spectra (XPS) measurements were performed in a PHI Quantum 2000 XPS system with a monochromatic Al Kα source and charge neutralizer to analyze surface chemicals and evaluate the amount and states of Nd atoms in the prepared samples. Nitrogen adsorption/desorption isotherms and Brunauer-Emmett-Teller (BET) specific surface area (S_{BET}) were recorded on a Micrometrics ASAP 2010 analyzer (accelerated surface area and porosimetry system). All the samples were treated at 100°C prior to BET measurements. Barret-Joyner-Halender (BJH) method was used to determine pore size distribution. The formation of hydroxyl radicals ($^\bullet$OH) on the surface of prepared samples under visible light was detected by a terephthalic acid (TA) probe method [17]. The PL spectra of generated 2-hydroxyterephthalic acid (TAOH) were measured by using a PerkinElmer Lambda 55 fluorescence spectrophotometer.

2.4. Photocatalytic Activity Measurement. The photocatalytic activities of the prepared samples were examined by the degradation of Rh-B under visible light. A 350 W Xenon lamp (Lap Pu, XQ) was used as a light source with a 420 nm cutoff filter right above the reactor to provide visible-light irradiation. The experiments were performed in self-constructed beaker-like glassware reactor with double walls for cooling system. 0.1 g of prepared sample was dispersed in 100 mL Rh-B solution with concentration of 10 μM. Prior to

irradiation, the solution was stirred in dark for 30 minutes to reach an adsorption/desorption equilibrium. Then, the solution was exposed to light while stirring. 1 mL suspension was collected every 30 minutes and was centrifuged for solid-liquid separation. Rh-B residue concentration was determined by measuring characteristic absorption intensity of Rh-B absorption spectrum over a Shimadzu UV-1700 UV-vis spectrophotometer.

Scavenger addition method [18] was used to explore the mechanism of photodegradation of Rh-B over Nd-doped TiO_2. The whole process was almost the same as that of the above photocatalytic activity measurement except with the presence of different scavengers: sodium oxalate ($Na_2Cr_2O_4$) as hole scavenger, KI as hole, and $^{\bullet}OH$ scavenger and $K_2Cr_2O_6$ (Cr (VI)) as electron scavenger.

3. Results and Discussion

3.1. Characterization of TiO_2 and Nd-Doped TiO_2 Photocatalysts. The degree of crystallinity and crystal structure of the prepared TiO_2 and Nd-doped TiO_2 samples were examined by XRD. The diffractograms recorded are shown in Figure 1. It reveals that the samples had anatase and brookite phases, a mixture of crystal structure. The phase content for the prepared samples is displayed in Table 1. With the increase in Nd doping amount, brookite phase content increased. In this study, the addition of NaOH to reaction solution increased pH value, leading to the increase of OH^- concentration. This might promote the formation of brookite phase because its complex consumed the amount of OH^- twice as much as rutile's one. However, too much NaOH could result in the formation of amorphous TiO_2 which contained much more OH^- than brookite complex [19–22]. The grain sizes of the prepared TiO_2 and Nd-doped TiO_2 powders were calculated using Scherrer equation:

$$D = \frac{K\lambda}{\beta \cos\theta}, \tag{1}$$

where D is crystalline size, λ the wavelength of X-ray radiation (0.1541 nm), K the constant usually taken as 0.89, and β the peak width at half-maximum height and θ diffraction angle. The obtained crystalline sizes are shown in Table 1. There was almost no change for crystallite size when Nd was incorporated (20.32 nm for pure TiO_2 and 20.35 nm for Nd-doped TiO_2 with Ti : Nd = 11 : 1). The phase content of TiO_2 can be calculated from the integrated intensities of anatase (101), rutile (101), and brookite (121) peaks with the following formulas [23]:

$$W_A = \frac{k_A A_A}{k_A A_A + A_R + k_B A_B},$$
$$W_R = \frac{A_R}{k_A A_A + A_R + k_B A_B}, \tag{2}$$
$$W_B = \frac{k_B A_B}{k_A A_A + A_R + k_B A_B},$$

where W_A, W_R, W_B represent the weight fractions of anatase, rutile, and brookite, respectively. The other symbols A_A, A_R, and A_B are the integrated intensities of anatase (101), rutile (110), and brookite (121) peaks, respectively. The variables k_A and k_B are two coefficients and their values are 0.886 and 2.721, respectively. The calculated data are shown in Table 1.

Substantially, the enlarged peaks at (101) (JCPDS number: 21-1272) and (121) plane for the three samples (Figures 1(B) and 1(C)) showed a slight shift to smaller angles with Nd incorporation. It indicates that Nd ion could enter into TiO_2 lattice or interstitial site. We know that the difference in ionic radius between neodymium ion (Nd^{3+} = 0.11 nm) and titanium ion (Ti^{4+} = 0.064 nm) is large. Without calcination treatment in high temperature, neodymium ions introduced by the coprecipitation-peptization method would unlikely enter into TiO_2 crystal structure. Actually, during $TiCl_4$ hydrolysis and peptization reaction, neodymium and oxygen ions could form Nd-O oxide on the superficial layer of TiO_2 [19, 20] particle by chemical bonding process and Nd^{3+} ions mainly existed as Nd–O–Ti in Nd-doped TiO_2 mixture [25]. So, the conversion from amorphous to well-crystalline structure usually requires high annealing temperature of at least 400°C.

The XRD studies revealed the anatase and brookite structure of the prepared samples. The formation of the structure was further confirmed by Raman spectroscopy. In Figure 2(A), Raman spectra of pure TiO_2 and Nd-doped TiO_2 are shown. It can be seen that the peaks observed at around 144.86, 398.17, 515.33, and 637.86 cm^{-1} were attributed to anatase TiO_2. The strongest Eg mode at 144.86 cm^{-1} arising from the external vibration of the anatase structure was well resolved, which indicates that anatase phase was formed in the as-prepared nanocrystals [24]. Its amplified figure is shown in Figure 2(B). It can be found that there was a distinct shift to high wave number after Nd doping, which is also an evidence to verify that Nd may be introduced into the lattice or interstitial site of titania. Additionally, there were three weak peaks at 240.22, 317.01, and 360.44 cm^{-1} attributed to vibration modes for brookite phase of TiO_2 in Figure 2(A). The absence of the characteristic vibration modes of Nd or Nd_2O_3 in the Raman spectra suggests that there was no Nd_2O_3 segregation into TiO_2.

The UV-Vis diffuse reflectance spectra (DRS) for the doped and the undoped TiO_2 nanoparticles samples are presented in Figure 3. Modification of TiO_2 with Nd significantly affected the light absorption property of the photocatalysts. A red shift of the absorption edge toward the visible region was observed for Nd-doped TiO_2 compared with pure TiO_2. From XRD and Raman data, we can see that Nd doping led to a little change of TiO_2 crystal structure and there was a little shift for the main peaks. The change of TiO_2 crystal structure may be due to the incorporation of Nd ion into TiO_2 lattice. It can result in new energy level in the bandgap and charge transfer between TiO_2 valence band and Nd ion doping level [21]. As a result, the Nd-doped TiO_2 had lower bandgap and the presence of Nd in the doped photocatalyst facilitated visible-light absorption. By plotting $(\alpha E)^{1/2}$ versus E with α the absorption coefficient, the bandgap was calculated to be 3.11 eV for pure TiO_2, 2.57 eV for Nd-doped TiO_2 with Ti : Nd = 23 : 1 and 2.33 eV

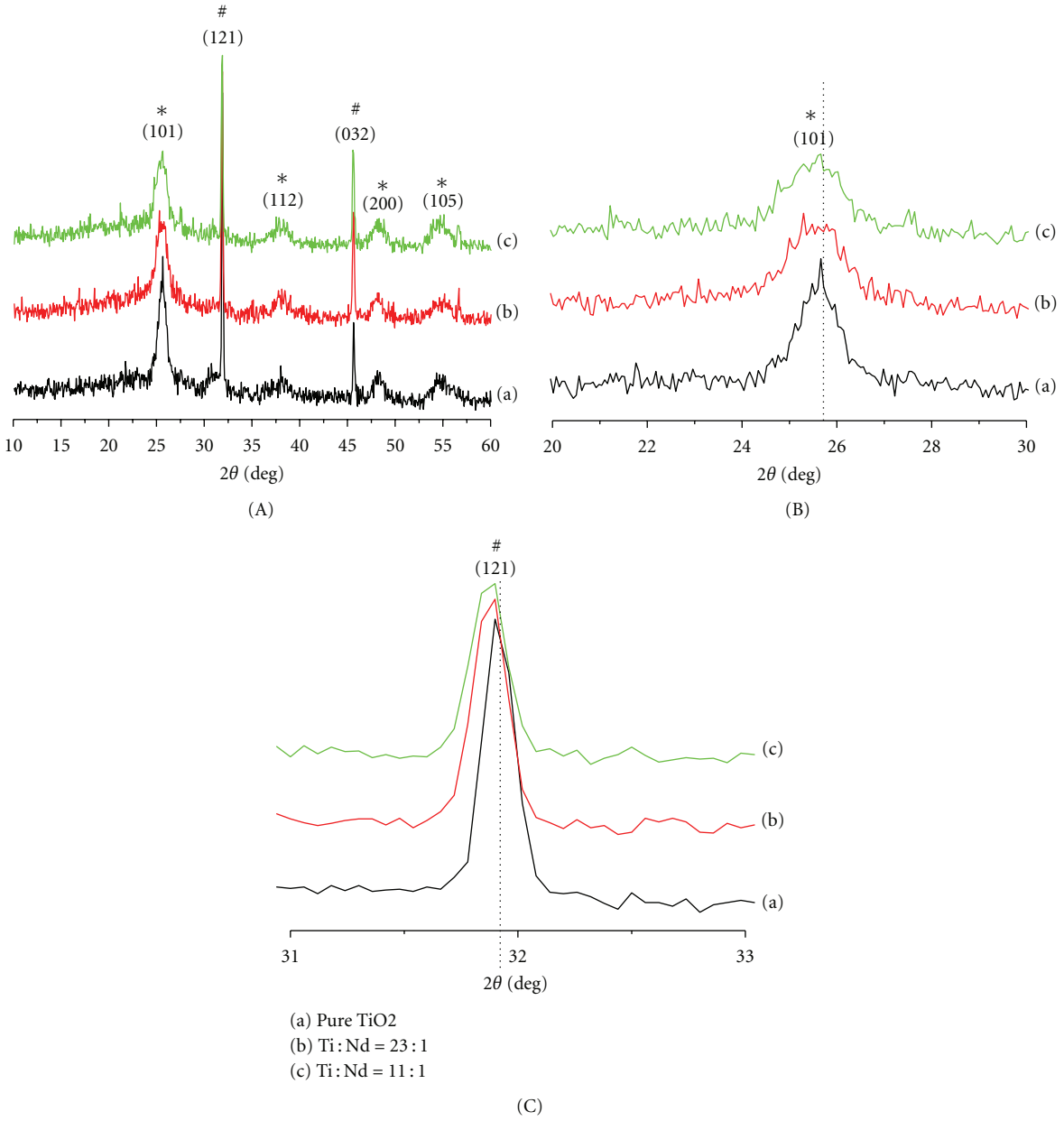

Figure 1: (A) XRD patterns of pure TiO_2 (a), Nd-doped TiO_2 with Ti : Nd = 23 : 1 (b), and Nd-doped TiO_2 with Ti : Nd = 11 : 1 (c). *anatase, #brookite. (B) The enlarged peak at (101) plane and (C) enlarged peak at (121) plane.

Table 1: Summary of the physicochemical properties of TiO_2 and Nd-doped TiO_2 composites.

Sample	Average size crystalline size (nm)[a]	Phase content[b] (%)		BET surface area ($m^2 \cdot g^{-1}$)	Pore size (nm)[c]	Total volume pore ($cm^3 \cdot g^{-1}$)	Bandgap (eV)
		Anatase	Brookite				
Pure TiO_2	20.32	13.97	86.02	72.46	3.54	0.172	3.11
Nd-doped TiO_2 (Ti : Nd = 23 : 1)	20.32	9.500	90.49	67.18	2.40	0.0830	2.57
Nd-doped TiO_2 (Ti : Nd = 11 : 1)	20.35	7.660	92.35	59.54	2.76	0.0831	2.33

[a] Determined by XRD using Scherrer equation based on (121) peak.
[b] Calculated using the formula in [24].
[c] Calculated from S_{BET}.

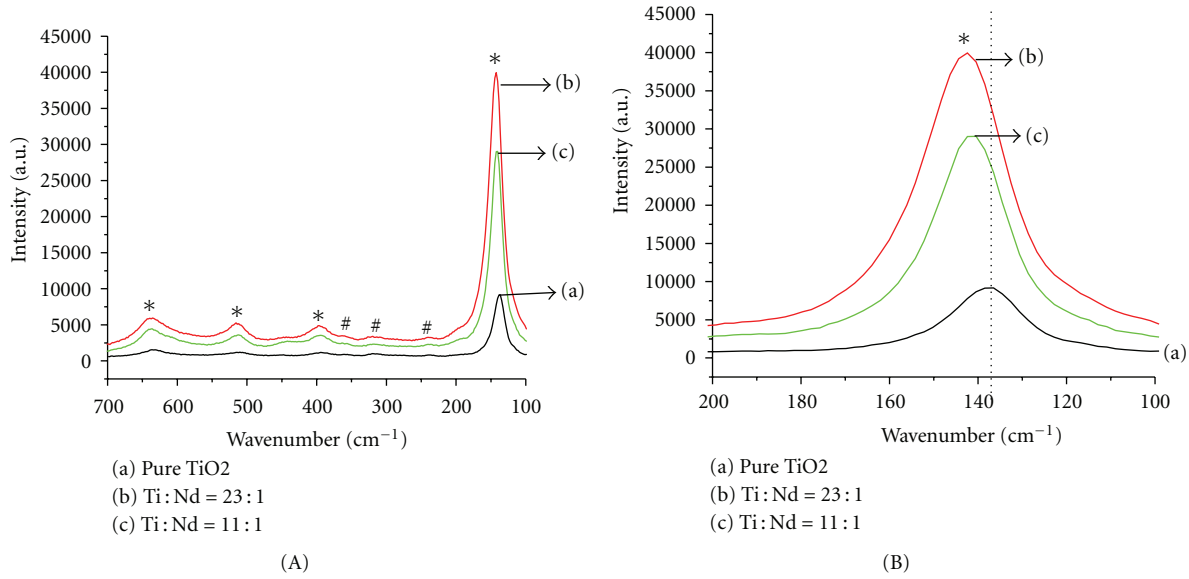

Figure 2: (A) Raman spectra of pure TiO_2 (a), Nd-doped TiO_2 with Ti : Nd = 23 : 1 (b), and Nd-doped TiO_2 with Ti : Nd = 11 : 1 (c). (B) The enlarged peak at 144.86 cm^{-1}.

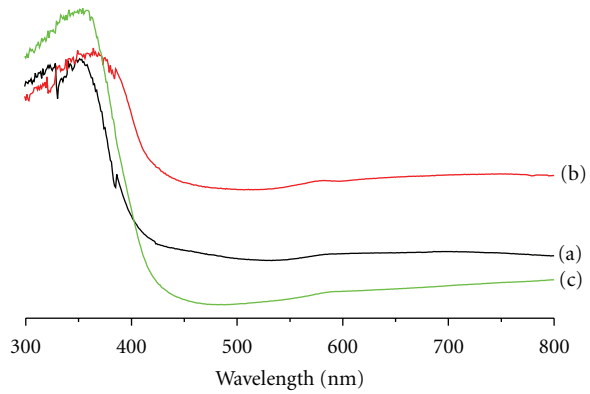

Figure 3: UV-Vis diffuse reflectance spectra of pure TiO_2 (a), Nd-doped TiO_2 with Ti : Nd = 23 : 1 (b), and Nd-doped TiO_2 with Ti : Nd = 11 : 1 (c).

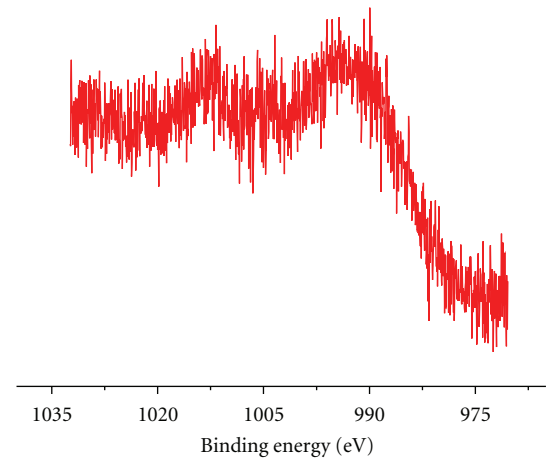

Figure 4: High-resolution XPS spectrum of Nd 3d for Nd-doped TiO_2 with Ti : Nd = 11 : 1.

for that with Ti : Nd = 11 : 1. So, with the presence of Nd ion in TiO_2 lattice, the bandgap of the materials decreased distinctly. Additionally, with the increase of Nd doping amount, the bandgap decreased gradually. It indicates that the Nd-doped TiO_2 samples may have the higher ability to absorb visible light.

XPS technique is used to investigate chemical component at the surface of a sample. Figure 4 shows high-resolution XPS spectrum for Nd in the doped TiO_2 sample. Although the peak for Nd was not so distinct, it can be confirmed that Nd was present in the doped sample. Figure 5 shows the high-resolution XPS spectrum for Ti 2p in pure TiO_2 and Nd-doped TiO_2 (Ti : Nd = 11 : 1) samples. The binding energy had 0.49 eV shift for Ti $2p_{3/2}$ and 0.65 eV for Ti $2p_{1/2}$, indicating the presence of Ti^{4+} and Ti^{3+}. Besides, the graph of doped sample was fitted by three subpeaks with the binding energy of 460.05, 458.86, and 458.27 eV, which indicates the presence of Ti^{4+}, Nd–Ti, and Ti^{3+}, respectively. So, the complete incorporation of Nd into TiO_2 lattice can be verified. The XPS spectra of the O 1s region of the pure TiO_2 could be fitted into two subpeaks at 529.36 and 531.08 eV (Figure 6(a)), corresponding to the Ti–O bond in TiO_2 and hydroxyl groups on the surface, respectively. However, the O 1s peak for Nd-doped TiO_2 was located at 530.21 eV and board. It could be fitted into three subpeaks at about 530.21, 531.34, and 532.84 eV (in Figure 6(b)), which can be ascribed to Ti–O, Nd–O, and hydroxyl group, respectively [26–28]. Therefore, three types of oxygen existed on the photocatalyst

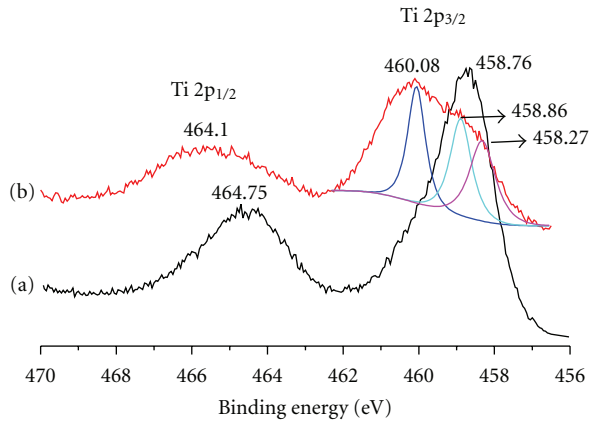

(a) Pure TiO2
(b) Ti : Nd = 11 : 1

Figure 5: High-resolution XPS spectra of Ti 2p for pure TiO_2 (a) and Nd-doped TiO_2 with Ti : Nd = 11 : 1 (b).

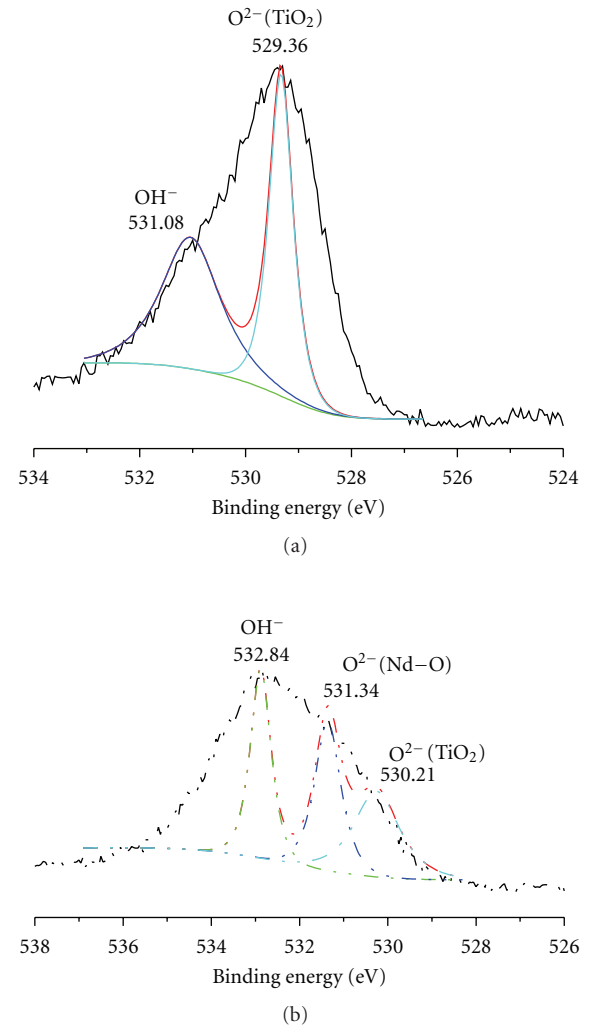

Figure 6: High-resolution XPS spectra of O 1s for pure TiO_2 (a) Nd-doped TiO_2 with Ti : Nd = 11 : 1 (b).

surface, including Ti–O in TiO_2, Nd–O, and hydroxyl group. These hydroxyl groups as hole trapped sites may inhibit the simple recombination of electron hole [29].

Surface textural characteristics of the samples pure TiO_2 and Nd-doped TiO_2 are derived from N_2 adsorption analysis. Specific surface area (S_{BET}) by BET method, total pore volume calculated at $P/P_0 = 0.99$, and average pore diameter values are presented in Table 1. The adsorption isotherms (Figure 7) of the samples showed type IV behaviour with the typical hysteresis loop. This hysteresis is characteristic of mesoporous materials [30, 31]. The pore size distributions for the pure TiO_2 and Nd-doped samples are shown in Figure 8, which confirms the mesoporous nature of the samples. It can be seen in Table 1 that the doped sample had lower surface area and narrower average pore size distribution than the undoped one. This might be due to the slight increase of crystalline size for the doped titania mentioned in XRD pattern.

3.2. Photocatalytic Activity of Prepared Samples. The photocatalytic property of titania is known to depend on several factors like crystallinity, phase assemblage, and surface area [32]. The photocatalytic activity of neodymium-doped and undoped titania was studied through Rh-B degradation under visible light in comparison with commercial product P25. Figure 9 shows the variations of Rh-B concentration against irradiation time with the presence of photocatalysts. It can be seen that the concentration of Rh-B decreased gradually with the exposure time for the pure and doped TiO_2 samples. Without the presence of photocatalysts, almost no Rh-B could be degraded. The results illustrate that all of the prepared samples had the ability for Rh-B degradation under visible light even for pure TiO_2 and P25. Additionally, with the increase of Nd doping amount, the photocatalytic activity for the Nd-doped TiO_2 increased. However, when the amount of Nd in the doped TiO_2 was too much (Ti : Nd $\geq$ 6 : 1), the activity was even lower than that of pure TiO_2 and P25. So, there is an optional Nd doping amount, which is in accordance with the published studies [14, 33]. Nevertheless, the optional Nd doping amount is 0.5% [14] and 1 ~ 3 wt% [33] in the two papers. The amount calculated by raw reagents for the formation of Nd-doped TiO_2 samples was about 9%, which is much higher. In fact, there should not be so much Nd incorporated into TiO_2 in this case. The measurement of actual Nd amount in TiO_2 is in progress.

3.3. Mechanism for Photocatalytic Activity Improvement by Nd Doping. From Figure 9, we can see that even pure TiO_2 could degrade Rh-B under visible light. It is known that Rh-B can be excited by visible light and inject electrons to the conduction band of TiO_2. So, the injected electrons react with O_2 molecules adsorbed on TiO_2 surface to yield $^{\bullet}O_2^-$ radical anion and subsequently $HO^{\bullet}$ radical by protonation [34]. So, in this case, Rh-B can be degraded in even undoped TiO_2 and P25 systems although their photodegradation efficiency is not high.

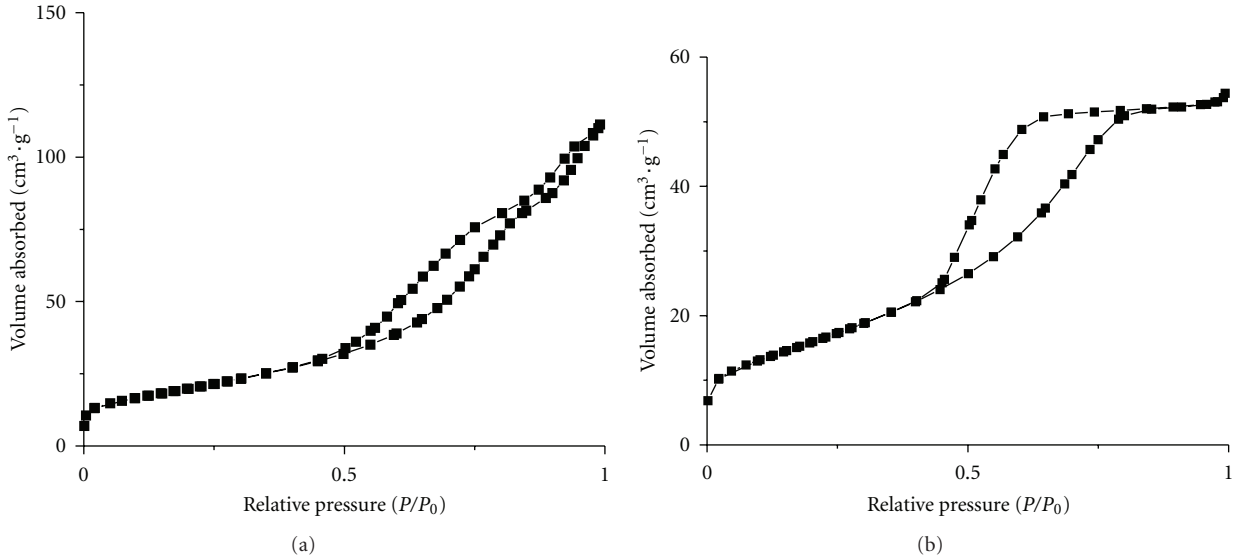

FIGURE 7: N_2 adsorption/desorption isotherms of pure TiO_2 (a) and Nd-doped TiO_2 with Ti : Nd = 11 : 1 (b).

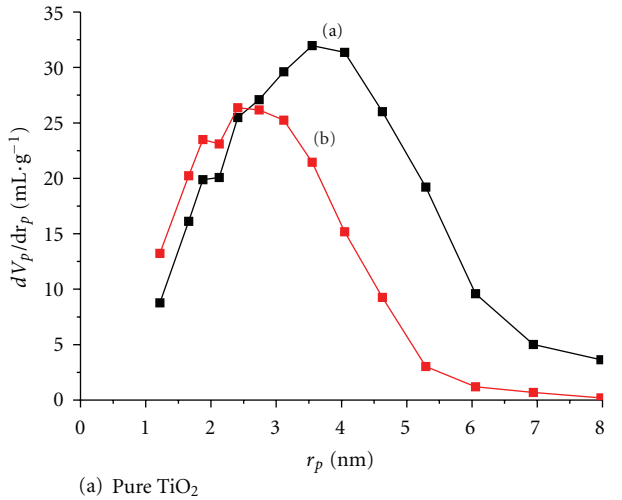

FIGURE 8: BJH pore size distribution curves for pure TiO_2 (a) and Nd-doped TiO_2 (Ti : Nd = 11 : 1) (b).

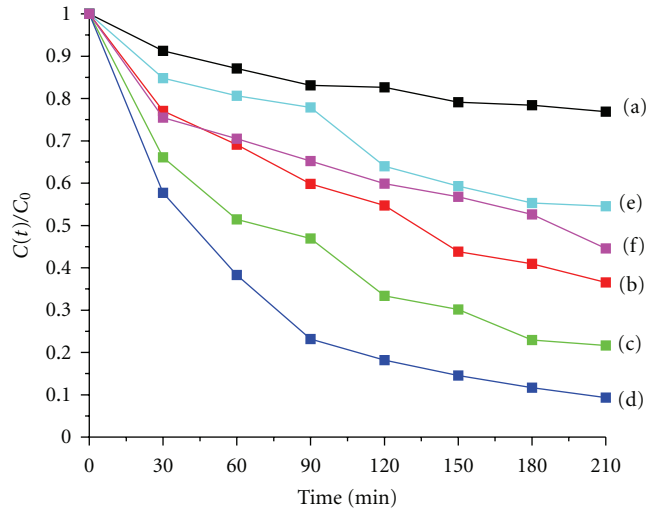

FIGURE 9: Photocatalytic degradation of Rh-B under visible light (solar simulator: 350 W Xenon lamp with a cutoff filter) with different conditions: (a) self degradation, (b) over pure TiO_2, (c) over Nd-doped TiO_2 with Ti : Nd = 23 : 1, (d) over Nd-doped TiO_2 with Ti : Nd = 11 : 1, (e) over Nd-doped TiO_2 with Ti : Nd = 6 : 1, and (f) over P25.

From Table 1 and Figure 7, we can see that the surface area of Nd-doped samples was lower than that of pure TiO_2 although all of them had mesoporous structure. So, based on dye and O_2 adsorption, there is no advantage for Nd doped samples compared with pure TiO_2. As discussed in the XRD patterns and XPS spectra, there is Nd which may substitute titanium in the lattice and exist as the state of Nd^{3+} although the ion radius of Nd^{3+} is much larger than that of Ti^{4+}. The doping energy level of Nd^{3+}/Nd^{2+} is −0.4 eV [35], which is more positive than the potential of conduction band of TiO_2 particles {E_{cb} = −0.5 eV versus NHE (normal hydrogen electrode) at pH = 1} [36]. Therefore, after Nd doing, the electrons can be excited from valance band to the Nd^{3+}/Nd^{2+}doping energy level under visible light. The UV-Vis spectra verifies that the Nd doped TiO_2 had lower bandgap than TiO_2 and was responsive to visible light (Figure 3). Besides, the energy of Nd^{3+}/Nd^{2+} is below the conduction band of TiO_2, so that it is easy for Nd^{3+} to capture injected electron by Rh-B from the conduction band. The electrons on the Nd^{3+}/Nd^{2+} level can react with O_2 adsorbed on TiO_2 surface to yield $^{\bullet}O_2^-$ radical anion and subsequently $HO^{\bullet}$ radical by protonation, just as the

electrons generated by Rh-B do. So, with the presence of part Nd in the lattice of TiO_2, there are more photogenerated electrons which participate in the formation of $^{\bullet}O_2^-$ radical anion and subsequently HO$^{\bullet}$ radical by protonation for dye degradation.

It can be seen from Figure 9 that the Nd-doped TiO_2 with Ti : Nd = 6 : 1 shows a negative effect on the photodegradation of Rh-B. In fact, metal ion dopant can act as a mediator of interfacial charge transfer or act as recombination center. So, there is an optimal value for dopant concentration [37]. Here, the doping energy level of Nd^{3+}/Nd^{2+} has three functions: firstly, it can capture electrons from the conduction band of TiO_2 that injected from the dye, and thus the number of hydroxide radicals is reduced; secondly, electrons can be excited to the Nd^{3+}/Nd^{2+} energy level from the valence band of TiO_2, and then the holes leaving on the valance band can degrade dyes; thirdly, Nd^{3+}/Nd^{2+} energy level can be the recombination center if the dopant concentration is not proper. These three processes compete with each other, so it is critical to find an optimal dopant concentration. In our experiment, from the result of photocatalytic activity, we can deduce that Nd doping concentration of 4 ~ 9 at. %, resulting in the good photocatalytic performance of Nd-doped TiO_2.

From the discussed above, we know that Nd doping level exists between bandgap of TiO_2 and is close to the conduction band, which corresponds to the calculation results [14]. So, with Nd-doped TiO_2 as a photocatalyst irradiated under visible light, there are photogenerated holes and electrons which participate in the Rh-B degradation. It is well known that in liquid photocatalysis system, hole may oxidize organic pollutant directly or form hydroxide radical for degradation, and photogenerated electron can form $^{\bullet}OH$ through the reaction with adsorbed $^{\bullet}O_2^-$. In order to explore which, photogenerated hole or electron, is mainly responsible for Rh-B degradation, some scavengers were used to investigate the specific reactive species that may play important roles in this process [18]. $Na_2Cr_2O_4$ was used as hole scavenger, KI as the scavenger for hole and $^{\bullet}OH$, and Cr (VI) for electron. Figure 10 shows the photodegradation efficiencies of Rh-B over Nd-doped TiO_2 (Ti : Nd = 11 : 1) in the presence of the scavengers under visible light. It can be seen that when $Na_2Cr_2O_4$ was used as diagnostic tool for suppressing the hole process, the photocatalytic degradation of Rh-B was inhibited but not down close to zero as shown in Figure 10. From this inhibited effect, it can be deduced that photogenerated holes played a role in the photodegradation of Rh-B under visible light. In the presence of KI as hole and $^{\bullet}OH$ scavenger, the removal efficiency of Rh-B was almost the same as that $Na_2Cr_2O_4$. It indicates that $^{\bullet}OH$ played a significant role in the system since the inhibition effect of $^{\bullet}OH$ can be regarded to be close to 100% after the deduction of hole effect. The addition of Cr (VI) as electron scavenger resulted in the degradation of only 6% of Rh-B after 90 min, which means that there was almost no activity for the photocatalyst with electron inhibition effect in the system. So, photogenerated electrons played a very important role in the degradation system. We know that the electrons resulted from Nd-doped TiO_2 and excited dye have strong reductive ability and they can reduce the

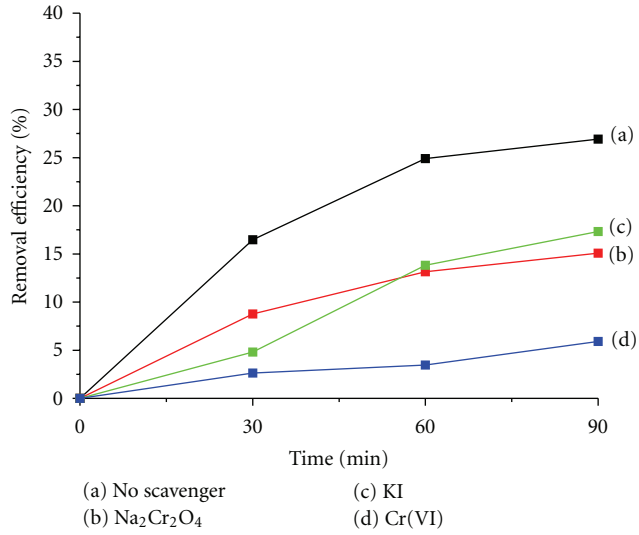

Figure 10: Photodegradation efficiencies of Rh-B (10 μM, 100 mL) over 0.1 g of Nd-doped TiO_2 with Ti : Nd = 11 : 1 under visible light with the presence of different scavengers, 5 mM sodium oxalate and KI, and 0.5 mM $K_2Cr_2O_6$.

adsorbed oxygen into $^{\bullet}O_2^-$ and then $^{\bullet}OH$ formation by protonation. These $^{\bullet}OH$ and $^{\bullet}O_2^-$ on the surface of the photocatalyst can degrade the adsorbed Rh-B [38]. From Figure 10, it can be concluded that $^{\bullet}O_2^-$ and $^{\bullet}OH$ are major reactive species for the photocatalytic degradation of Rh-B, and photogenerated electrons from Nd-doped TiO_2 are responsible for the improvement of photocatalytic activity of the Nd-doped TiO_2.

In order to verify that $^{\bullet}OH$ is present in the photodegradation system, the changes of PL spectra of terephthalic acid solution with irradiation time were recorded and the data is shown in Figure 11. It can be seen that a gradual increase in PL intensity at about 430 nm was observed with the increase of irradiation time. However, no PL increase was observed in the absence of visible light or Nd-doped TiO_2 sample. This suggests that the fluorescence is from the chemical reaction between terephthalic acid and $^{\bullet}OH$ formed via photogenerated holes and electrons. Usually, PL intensity is proportional to the amount of produced hydroxyl radical over the photocatalyst [38]. So, the amount of formed hydroxyl radical gradually increased for Rh-B degradation under visible light with the increase of time.

Moreover, since the radius of Nd^{3+} is much larger than that of Ti^{4+}, it will be difficult for all of Nd ions added to enter into TiO_2 lattice. So, the presence of Nd^{3+} or Nd metal on nanoparticle surface may also promote the charge separation to improve photocatalytic activity of Nd-doped TiO_2, which has been described by many published papers [14, 39–43].

4. Conclusion

In summary, a simple sol-gel method has been used for the preparation of Nd-doped titania nanoparticles with anatase and brookite phases. The prepared samples can

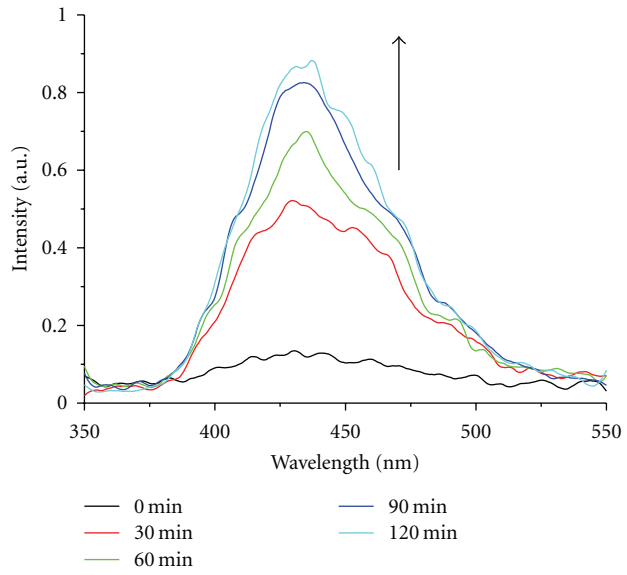

Figure 11: PL spectral changes with irradiation time over Nd-doped TiO_2 with Ti : Nd = 11 : 1 in terephthalic acid solution of 5×10^{-4} M.

achieve photocatalytic degradation of dye (Rh-B) under visible light, and Nd-doped TiO_2 has better activity than pure TiO_2 and P25. The enhanced activity is related to the change of crystalline structure of TiO_2. Partial Nd enters into TiO_2 lattice for the formation of doping level, which makes TiO_2 responsive to visible light. In Rh-B degradation system, hydroxide radicals as one of the reactive species are mainly produced by photogenerated electrons both from dye and Nd-doped TiO_2 excitation and they are responsible for Rh-B degradation. The contribution from hole is not as pronounced as electron for the formation of hydroxide radials. This study may shed light on the improvement of photocatalytic activity of TiO_2 under solar light by using metal doping method.

Acknowledgments

This work was financially supported by the National Natural Science Foundation of China (no. 20973070), the National Basic Research Program of China (no. 2009CB939704), the Key Project of the Ministry of Chinese Education (no. 109116), self-determined research funds of CCNU from the colleges' basic research, Natural Science Foundation of Jiangsu Province (no. BK2009724), and Industry R&D program in Zhenjiang City (no. GY2009003). The authors are also indebted to Professor Wen-Zhong Shen and Miss Dan-Hua Xu in Shanghai Jiaotong University for Raman spectrum measurements.

References

[1] Y. Xie, C. Yuan, and X. Li, "Photocatalytic degradation of X-3B dye by visible light using lanthanide ion modified titanium dioxide hydrosol system," *Colloids and Surfaces A*, vol. 252, no. 1, pp. 87–94, 2005.

[2] Q. Xiang, J. Yu, W. Wang, and M. Jaroniec, "Nitrogen self-doped nanosized TiO_2 sheets with exposed 001 facets for enhanced visible-light photocatalytic activity," *Chemical Communications*, vol. 47, no. 24, pp. 6906–6908, 2011.

[3] Q. Xiang, J. Yu, and M. Jaroniec, "Nitrogen and sulfur co-doped TiO_2 nanosheets with exposed 001 facets: synthesis, characterization and visible-light photocatalytic activity," *Physical Chemistry Chemical Physics*, vol. 13, no. 11, pp. 4853–4861, 2011.

[4] J. Yu, G. Dai, Q. Xiang, and M. Jaroniec, "Fabrication and enhanced visible-light photocatalytic activity of carbon self-doped TiO_2 sheets with exposed 001 facets," *Journal of Materials Chemistry*, vol. 21, no. 4, pp. 1049–1057, 2011.

[5] G. Shang, S. Yang, T. Xu, and H. Fu, "Mechanistic study of visible-Light-induced photodegradation of 4-chlorophenol by TiO_2-xNx ($0.021<x<0.049$) with low nitrogen concentration," *International Journal of Photoenergy*, vol. 2012, Article ID 759306, 9 pages, 2012.

[6] N.-H. Lee, H.-J. Oh, S.-C. Jung, W.-J. Lee, D.-H. Kim, and S.-J. Kim, "Photocatalytic properties of nanotubular-shaped TiO_2 powders with anatase phase obtained from titanate nanotube powder through various thermal treatments," *International Journal of Photoenergy*, vol. 2011, Article ID 327821, 7 pages, 2011.

[7] F. Nerud, P. Baldrian, J. Gabriel, and D. Ogbeifun, "Decolorization of synthetic dyes by the Fenton reagent and the Cu/pyridine/H_2O_2 system," *Chemosphere*, vol. 44, no. 5, pp. 957–961, 2001.

[8] X. Chen, L. Liu, P. Y. Yu, and S. S. Mao, "Increasing solar absorption for photocatalysis with black hydrogenated titanium dioxide nanocrystals," *Science*, vol. 746, pp. 747–749, 2011.

[9] M. Ksibi, S. B. Amor, S. Cherif, E. Elaloui, A. Houas, and M. Elaloui, "Photodegradation of lignin from black liquor using a UV/TiO_2 system," *Journal of Photochemistry and Photobiology A*, vol. 154, no. 2-3, pp. 211–218, 2003.

[10] J. Xie, D. Jiang, M. Chen et al., "Preparation and characterization of monodisperse Ce-doped TiO_2 microspheres with visible light photocatalytic activity," *Colloids and Surfaces A*, vol. 372, no. 1–3, pp. 107–114, 2010.

[11] X. Wu, P. Su, H. Liu, and L. Qi, "Photocatalytic degradation of Rhodamine B under visible light with Nd-doped titanium dioxide films," *Journal of Rare Earths*, vol. 27, no. 5, pp. 739–743, 2009.

[12] S. Suárez, T. L. R. Hewer, R. Portela, M. D. Hernández-Alonso, R. S. Freire, and B. Sánchez, "Behaviour of TiO_2-SiMgOx hybrid composites on the solar photocatalytic degradation of polluted air," *Applied Catalysis B*, vol. 101, no. 3-4, pp. 176–182, 2011.

[13] H. Kisch and W. Macyk, "Visible-light photocatalysis by modified titania," *ChemPhysChem*, vol. 3, no. 5, pp. 399–400, 2002.

[14] D. Zhao, T. Peng, J. Xiao, C. Yan, and X. Ke, "Preparation, characterization and photocatalytic performance of Nd^{3+}-doped titania nanoparticles with mesostructure," *Materials Letters*, vol. 61, no. 1, pp. 105–110, 2007.

[15] V. Štengl, S. Bakardjieva, and N. Murafa, "Preparation and photocatalytic activity of rare earth doped TiO_2 nanoparticles," *Materials Chemistry and Physics*, vol. 114, no. 1, pp. 217–226, 2009.

[16] A. L. Linsebigler, G. Lu, and J. T. Yates, "Photocatalysis on TiO_2 surfaces: principles, mechanisms, and selected results," *Chemical Reviews*, vol. 95, no. 3, pp. 735–758, 1995.

[17] Z. M. Wang, G. Yang, P. Biswas, W. Bresser, and P. Boolchand, "Processing of iron-doped titania powders in flame aerosol reactors," *Powder Technology*, vol. 114, no. 1–3, pp. 197–204, 2001.

[18] L.-S. Zhang, K.-H. Wong, H.-Y. Yip et al., "Effective photocatalytic disinfection of *E. coli* K-12 using AgBr-Ag-Bi 2WO6 nanojunction system irradiated by visible light: the role of diffusing hydroxyl radicals," *Environmental Science and Technology*, vol. 44, no. 4, pp. 1392–1398, 2010.

[19] K. V. Baiju, P. Periyat, W. Wunderlich, P. Krishna Pillai, P. Mukundan, and K. G. K. Warrier, "Enhanced photoactivity of neodymium doped mesoporous titania synthesized through aqueous sol-gel method," *Journal of Sol-Gel Science and Technology*, vol. 43, no. 3, pp. 283–290, 2007.

[20] A. L. Castro, M. R. Nunes, M. D. Carvalho et al., "Doped titanium dioxide nanocrystalline powders with high photocatalytic activity," *Journal of Solid State Chemistry*, vol. 182, no. 7, pp. 1838–1845, 2009.

[21] X. Su, J. Zhao, Y. Li et al., "Solution synthesis of Cu_2O/TiO_2 core-shell nanocomposites," *Colloids and Surfaces A*, vol. 349, no. 1–3, pp. 151–155, 2009.

[22] W. Xue, G. Zhang, X. Xu, X. Yang, C. Liu, and Y. Xu, "Preparation of titania nanotubes doped with cerium and their photocatalytic activity for glyphosate," *Chemical Engineering Journal*, vol. 167, no. 1, pp. 397–402, 2011.

[23] H. Zhang and J. F. Banfield, "Understanding polymorphic phase transformation behavior during growth of nanocrystalline aggregates: insights from TiO_2," *Journal of Physical Chemistry B*, vol. 104, no. 15, pp. 3481–3487, 2000.

[24] Y. Yu, J. C. Yu, J. G. Yu et al., "Enhancement of photocatalytic activity of mesoporous TiO_2 by using carbon nanotubes," *Applied Catalysis A*, vol. 289, no. 2, pp. 186–196, 2005.

[25] Y. Lv, L. Yu, H. Huang, H. Liu, and Y. Feng, "Preparation of F-doped titania nanoparticles with a highly thermally stable anatase phase by alcoholysis of $TiCl_4$," *Applied Surface Science*, vol. 255, no. 23, pp. 9548–9552, 2009.

[26] T. L. R. Hewer, E. C. C. Souza, T. S. Martins, E. N. S. Muccillo, and R. S. Freire, "Influence of neodymium ions on photocatalytic activity of TiO_2 synthesized by sol-gel and precipitation methods," *Journal of Molecular Catalysis A*, vol. 336, no. 1-2, pp. 58–63, 2011.

[27] Y. H. Xu, C. Chen, X. L. Yang, X. Li, and B. F. Wang, "Preparation, characterization and photocatalytic activity of the neodymium-doped TiO_2 nanotubes," *Applied Surface Science*, vol. 255, no. 20, pp. 8624–8628, 2009.

[28] U. I. Gaya and A. H. Abdullah, "Heterogeneous photocatalytic degradation of organic contaminants over titanium dioxide: a review of fundamentals, progress and problems," *Journal of Photochemistry and Photobiology C*, vol. 9, no. 1, pp. 1–12, 2008.

[29] J. W. Shi, "Preparation of Fe(III) and Ho(III) co-doped TiO_2 films loaded on activated carbon fibers and their photocatalytic activities," *Chemical Engineering Journal*, vol. 151, no. 1–3, pp. 241–246, 2009.

[30] W. Ho, J. C. Yu, J. Lin, J. Yu, and P. Li, "Preparation and photocatalytic behavior of MoS_2 and WS_2 nanocluster sensitized TiO_2," *Langmuir*, vol. 20, no. 14, pp. 5865–5869, 2004.

[31] S. J. Greegg and K. S. W. Sing, *Adsorption, Surface Area and Porosity*, Academic Press, London, UK, 2nd edition, 1982.

[32] J. Xu, M. Chen, and D. Fu, "Study on highly visible light active Bi-doped TiO_2 composite hollow sphere," *Applied Surface Science*, vol. 257, no. 17, pp. 7381–7386, 2011.

[33] S. Rengaraj, S. Venkataraj, J. W. Yeon, Y. Kim, X. Z. Li, and G. K. H. Pang, "Preparation, characterization and application of Nd-TiO_2 photocatalyst for the reduction of Cr(VI) under UV light illumination," *Applied Catalysis B*, vol. 77, no. 1-2, pp. 157–165, 2007.

[34] T. Wu, G. Liu, J. Zhao, H. Hidaka, and N. Serpone, "Photoassisted degradation of dye pollutants. V. Self-photosensitized oxidative transformation of Rhodamine B under visible light irradiation in aqueous TiO_2 dispersions," *Journal of Physical Chemistry B*, vol. 102, no. 30, pp. 5845–5851, 1998.

[35] Y. Xie, C. Yuan, and X. Li, "Photosensitized and photocatalyzed degradation of azo dye using Ln^{n+}-TiO_2 sol in aqueous solution under visible light irradiation," *Materials Science and Engineering B*, vol. 117, no. 3, pp. 325–333, 2005.

[36] C. Chen, X. Li, W. Ma, J. Zhao, H. Hidaka, and N. Serpone, "Effect of transition metal ions on the TiO_2-assisted photodegradation of dyes under visible irradiation: a probe for the interfacial electron transfer process and reaction mechanism," *Journal of Physical Chemistry B*, vol. 106, no. 2, pp. 318–324, 2002.

[37] Y. Cong, J. Zhang, F. Chen, M. Anpo, and D. He, "Preparation, photocatalytic activity, and mechanism of nano-TiO_2 Co-doped with nitrogen and iron (III)," *Journal of Physical Chemistry C*, vol. 111, no. 28, pp. 10618–10623, 2007.

[38] J. Yu, Q. Xiang, and M. Zhou, "Preparation, characterization and visible-light-driven photocatalytic activity of Fe-doped titania nanorods and first-principles study for electronic structures," *Applied Catalysis B*, vol. 90, no. 3-4, pp. 595–602, 2009.

[39] W. Choi, A. Termin, and M. R. Hoffmann, "The role of metal ion dopants in quantum-sized TiO_2: correlation between photoreactivity and charge carrier recombination dynamics," *Journal of Physical Chemistry*, vol. 98, no. 51, pp. 13669–13679, 1994.

[40] S. Rengaraj and X. Z. Li, "Enhanced photocatalytic reduction reaction over Bi^{3+}-TiO_2 nanoparticles in presence of formic acid as a hole scavenger," *Chemosphere*, vol. 66, no. 5, pp. 930–938, 2007.

[41] N. Serpone, "Is the band gap of pristine TiO_2 narrowed by anion- and cation-doping of titanium dioxide in second-generation photocatalysts?" *Journal of Physical Chemistry B*, vol. 110, no. 48, pp. 24287–24293, 2006.

[42] J.-M. Herrmann, H. Tahiri, Y. Ait-Ichou, G. Lassaletta, A. R. González-Elipe, and A. Fernandez, "Characterization and photocatalytic activity in aqueous medium of TiO_2 and Ag-TiO_2 coatings on quartz," *Applied Catalysis B*, vol. 13, no. 3-4, pp. 219–228, 1997.

[43] A. Sclafani and J.-M. Herrmann, "Influence of metallic silver and of platinum-silver bimetallic deposits on the photocatalytic activity of titania (anatase and rutile) in organic and aqueous media," *Journal of Photochemistry and Photobiology A*, vol. 113, no. 2, pp. 181–188, 1998.